UCSF
UC San Francisco Previously Published Works

Title

IL-7 receptor blockade reverses autoimmune diabetes by promoting inhibition of effector/memory T cells

Permalink

https://escholarship.org/uc/item/7598t58t

Journal

Proceedings of the National Academy of Sciences of the United States of America, 109(31)

ISSN

0027-8424

Authors

Penaranda, Cristina
Kuswanto, Wilson
Hofmann, Jerry
et al.

Publication Date

2012-07-31

DOI

10.1073/pnas.1203692109

Peer reviewed

eScholarship.org Powered by the California Digital Library
University of California

IL-7 receptor blockade reverses autoimmune diabetes by promoting inhibition of effector/memory T cells

Cristina Penaranda[a], Wilson Kuswanto[b], Jerry Hofmann[b], Rupert Kenefeck[c], Parth Narendran[c], Lucy S. K. Walker[c], Jeffrey A. Bluestone[a], Abul K. Abbas[b], and Hans Dooms[b,1,2]

[a]Diabetes Center and [b]Department of Pathology, University of California, San Francisco, CA 94143; and [c]School of Immunity and Infection, University of Birmingham Medical School, Birmingham B15 2TT, United Kingdom

Edited* by Lewis L. Lanier, University of California, San Francisco, CA, and approved May 28, 2012 (received for review March 2, 2012)

To protect the organism against autoimmunity, self-reactive effector/memory T cells ($T_{E/M}$) are controlled by cell-intrinsic and -extrinsic regulatory mechanisms. However, how some $T_{E/M}$ cells escape regulation and cause autoimmune disease is currently not understood. Here we show that blocking IL-7 receptor-α (IL-7Rα) with monoclonal antibodies in nonobese diabetic (NOD) mice prevented autoimmune diabetes and, importantly, reversed disease in new-onset diabetic mice. Surprisingly, IL-7–deprived diabetogenic $T_{E/M}$ cells remained present in the treated animals but showed increased expression of the inhibitory receptor Programmed Death 1 (PD-1) and reduced IFN-γ production. Conversely, IL-7 suppressed PD-1 expression on activated T cells in vitro. Adoptive transfer experiments revealed that $T_{E/M}$ cells from anti–IL-7Rα–treated mice had lost their pathogenic potential, indicating that absence of IL-7 signals induces cell-intrinsic tolerance. In addition to this mechanism, IL-7Rα blockade altered the balance of regulatory T cells and $T_{E/M}$ cells, hence promoting cell-extrinsic regulation and further increasing the threshold for diabetogenic T-cell activation. Our data demonstrate that IL-7 contributes to the pathogenesis of autoimmune diabetes by enabling $T_{E/M}$ cells to remain in a functionally competent state and suggest IL-7Rα blockade as a therapy for established T-cell–dependent autoimmune diseases.

type 1 diabetes | cytokines | immune regulation

Type 1 diabetes is an autoimmune disease caused by a gradual lymphocytic infiltration of the pancreas that leads to the destruction of the insulin-producing β-cells in the islets of Langerhans. Autoreactive $CD4^+$ T cells are known to be essential for the initiation and progression of islet infiltration and, ultimately, the destruction of β-cells, resulting in insufficient islet mass to control blood-sugar levels (1). However, the signals and mechanisms that enable autoreactive T cells to overcome the various inhibitory and tolerance mechanisms that operate to protect the organism from autoimmune disease are poorly understood.

IL-7 has long been recognized as an essential cytokine for naïve and memory T-cell homeostasis (2); however, recent studies are expanding its functions, showing that administration of IL-7 increases effector functions in tumor-specific and antiviral $CD8^+$ T cells by counteracting various suppressive mechanisms (3, 4). In these models, a reduction in T cells expressing the inhibitory cell-surface receptor Programmed Death 1 (PD-1) (5–7) was observed and this correlated with improved antitumor responses and viral clearance. In nonobese diabetic (NOD) mice, interaction of PD-1 with its ligand PD-L1, which is expressed on lymphocytes and β-cells, strongly protects against autoimmune diabetes (8, 9), and this mechanism also maintains islet tolerance in therapeutic models (10, 11). Taken together, these studies raise the possibility that physiological levels of IL-7 allow a fraction of diabetogenic T cells to escape inhibitory mechanisms, such as the PD-1/PD-L1 pathway and, as a consequence, that blocking IL-7 may be of therapeutic benefit in type 1 diabetes.

To define the role of IL-7 in diabetes, we blocked IL-7 signals with anti–IL-7 receptor α (IL-7Rα) mAbs in NOD mice and found that this treatment not only prevented the development of diabetes, but also reversed established disease. Based on the role of IL-7 as a T-cell survival factor, we predicted that the underlying mechanism for this therapy would be depletion of islet-reactive effector/memory T cells ($T_{E/M}$) cells. However, the antibody treatment did not lead to robust depletion of $T_{E/M}$ cells and islet infiltrates remained significant. Our data show that IL-7Rα blockade increased the proportion of PD-1–expressing $T_{E/M}$ cells and regulatory T cells (Tregs). Although both these mechanisms likely contribute to the therapeutic effect, we demonstrate a unique physiological function of IL-7 in autoreactive T cells, namely to suppress PD-1–mediated inhibition enabling them to become pathogenic $T_{E/M}$ cells.

Results

IL-7Rα Blockade Prevents and Reverses Autoimmune Diabetes. IL-7 is a critical cytokine for the generation and maintenance of virus-specific memory T cells, but its role in autoimmune disease is poorly defined. One of the challenges in treating autoimmune type 1 diabetes is that it is a slowly developing chronic disease, and the efficacy of most treatments highly depends on the stage of the disease at which the treatment is given (12). To assess whether blocking IL-7 signals in NOD mice would interfere with disease development, we administered anti–IL-7Rα mAbs to block IL-7 cytokine activity. For the first set of experiments, we started treating prediabetic NOD mice with anti–IL-7Rα mAbs at 10 wk of age, when islet infiltration is established. In control groups, mice started becoming diabetic at age 14 wk and, as expected, the incidence of diabetes gradually increased over the treatment period, reaching 60–70% by 24 wk. In contrast, only 10% of mice receiving anti–IL-7Rα antibodies developed diabetes during the treatment period (Fig. 1*A*). Protection from disease was accompanied by diminished, but not absent, islet infiltration in the treated animals (Fig. 1 *B* and *C*), as determined by histological examination. These results show that IL-7 is essential for the development of the anti-islet response, and blocking this cytokine compromises the generation, survival, and function of pathogenic, islet-reactive T cells.

Although this result established a role for IL-7 in disease development, it is clinically more relevant to initiate treatment once hyperglycemia is apparent. To test whether blocking IL-7 could reverse established diabetes, we administered anti–IL-7Rα mAbs to a cohort of new-onset diabetic NOD mice and followed blood-glucose levels. We found that this treatment restored normoglycemia in ∼50% of treated animals (Fig. 1*D*). Importantly, anti–IL-7Rα–treated mice remained normoglycemic long after the treatment was stopped, far exceeding the estimated half-life of the antibodies. The eventual relapse is likely caused by newly activated naïve islet-specific T cells that remained

Author contributions: C.P., L.S.K.W., J.A.B., A.K.A., and H.D. designed research; C.P., W.K., J.H., R.K., P.N., and H.D. performed research; C.P., W.K., R.K., L.S.K.W., and H.D. analyzed data; and H.D. wrote the paper.

The authors declare no conflict of interest.

*This Direct Submission article had a prearranged editor.

See Commentary on page 12270.

[1]To whom correspondence should be addressed. E-mail: hdooms@bu.edu.

[2]Present address: Boston University School of Medicine, Arthritis Center/Rheumatology, 72 East Concord Street, E-5, Boston, MA 02118.

This article contains supporting information online at www.pnas.org/lookup/suppl/doi:10.1073/pnas.1203692109/-/DCSupplemental.

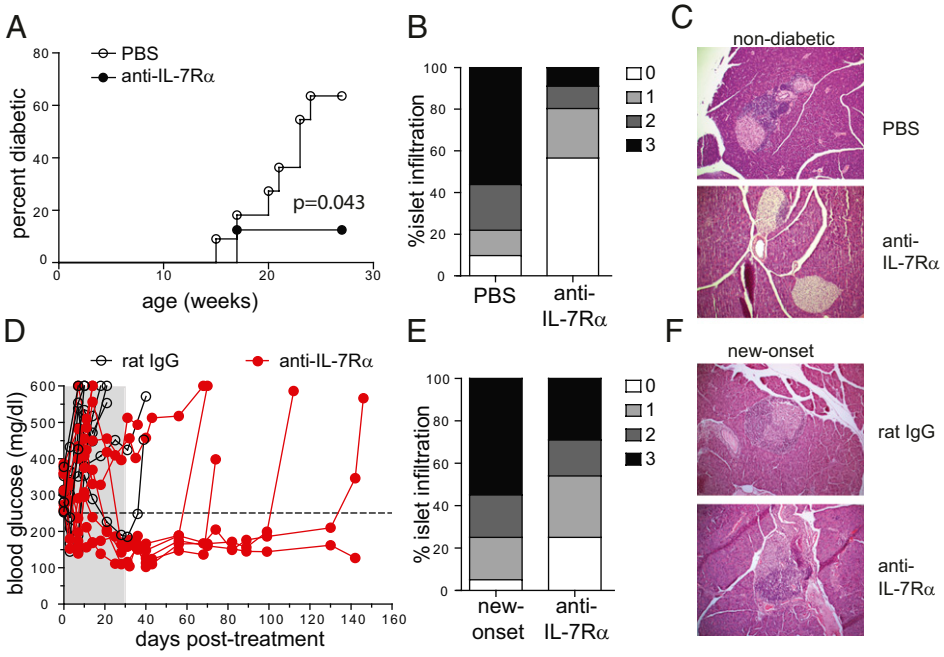

Fig. 1. IL-7Rα blockade prevents and reverses diabetes in NOD mice. (*A*) Female NOD mice were treated with anti–IL-7Rα monoclonal antibodies (n = 8) or PBS (n = 11) for 14 wk, starting at 10 wk of age, and diabetes incidence was followed. (*B*) Infiltration of pancreatic islets in 24-wk-old nondiabetic mice from *A* quantified as percentages of islets showing the indicated histological scores (see *Materials and Methods*) (PBS, n = 3; anti–IL-7Rα, n = 6). (*C*) Representative pictures of islets in 24-wk-old, nondiabetic mice from *A* at 20× magnification. (*D*) New-onset diabetic NOD mice [blood glucose between 250–400 mg/dL (dotted line)] were treated with anti–IL-7Rα antibodies (n = 10) or rat IgG (n = 9) for 4 wk (shaded area). Blood-glucose levels were followed for up to 5 mo. (*E*) Histological scores of new-onset NOD mice that became normoglycemic after anti–IL-7Rα treatment compared with untreated new-onset mice. (*F*) Representative pictures of islets in new-onset mice or mice cured after anti–IL-7Rα treatment at 20× magnification.

present in the lymphoid organs or recently emigrated from the thymus. Our results add IL-7Rα blockade to the list of only a handful of treatments capable of reversing the disease (12) and is unique as a cytokine receptor blockade therapy for the treatment of autoimmune diabetes. Surprisingly, histological analysis showed only a limited reduction of the islet infiltrates (Fig. 1 *E* and *F*), suggesting that rapid and robust depletion of islet-reactive T cells may not be the mechanism of IL-7Rα blockade therapy.

IL-7Rα Blockade Does Not Specifically Deplete Islet-Specific $T_{E/M}$ Cells. Given the well-established role of IL-7 in regulating T-cell survival and homeostasis (2), we evaluated cell numbers in the pancreatic and inguinal lymph nodes and spleens of anti–IL-7Rα–treated NOD mice. Not surprisingly, both total lymphocyte (Fig. S1*A*) and $CD4^+$ T cells numbers (Fig. S1 *B* and *C*) showed a tendency to decrease after 2–4 wk of anti–IL-7Rα treatment. The A7R34 antibody clone (13) we used in this study is a rat IgG2a isotype that does not cause antibody-dependent cell-mediated cytotoxicity (14), and hence the observed effects can be specifically attributed to blocking IL-7 signals.

Two possible explanations for the long-lasting therapeutic effect seen after IL-7Rα blockade are: (*i*) within the $CD4^+$ T-cell population, islet antigen-specific $T_{E/M}$ cells were more sensitive to the absence of IL-7 and their survival was preferentially compromised, or (*ii*) the treatment induced tolerance in diabetogenic T cells. Diabetogenic $CD4^+$ T cells in the NOD mouse can be identified in adoptive transfer experiments (15) and are predominantly found in the $CD44^{high}$ $T_{E/M}$ cell population (16, 17). Analysis of $CD44^{high}$ $T_{E/M}$ cells showed that the proportion of this population within $CD4^+$ T cells, excluding $Foxp3^+$ Tregs, increased over time in anti–IL-7Rα–treated mice (Fig. 2*A*), suggesting that the main population affected by IL-7Rα blockade is naïve T cells, which express intermediate levels of IL-7Rα. Because of the general decrease in $CD4^+$ T cells (Fig. S1*C*), absolute numbers of $CD44^{high}$ cells didn't show an increase on day 16 of anti–IL-7Rα vs. rat IgG treatment: averages were respectively 290,474 vs. 299,552 [pancreatic lymph nodes (PLNs)]; 211,941 vs. 426,953 [inguinal lymph nodes (ILNs)], and 2,253,943 vs. 2,902,614 (spleen). The $CD44^{high}$ $T_{E/M}$ population consists of IL-7Rα^{low} effector cells and IL-7Rα^{high} memory cells (18–20). To directly rule out that IL-7Rα blockade led to selective deletion of $CD44^{high}$ IL-7Rα^{high} memory T cells, we stained $CD4^+$ T-cell populations from isotype and anti–IL-7Rα–treated mice with fluorescently labeled anti-rat Ig secondary antibodies to detect cells whose surface was coated with anti–IL-7Rα antibodies in vivo. Interestingly, both $CD44^{high}$IL-7Rα^{high} memory and $CD44^{high}$IL-7Rα^{low} effector cells were readily detected, and no selective elimination of memory cells was observed in comparison with isotype-treated controls (Fig. 2*B*). Hence, although absolute numbers of memory T cells decrease to some extent, their relative presence in the $CD4^+$ T-cell population was not diminished by IL-7 deprivation. To further characterize the impact of blocking anti–IL-7Rα antibodies on the homeostasis of naïve and memory T cells, congenically marked naïve and memory T cells from NOD mice were labeled with the cell division tracker carboxyfluorescein diacetate succinimidyl ester (CFSE) and adoptively transferred to new NOD recipients. We followed their survival and proliferation after IL-7Rα blockade and, remarkably, found no differences in the percentages of naïve and memory T cells (Fig. 2*C*). Moreover, although naïve T cells did not significantly divide in the hosts, memory T-cell proliferation—likely driven by autoantigens—could not be blocked with anti–IL-7Rα antibodies.

Finally, to exclude the possibility that IL-7Rα blockade selectively depleted islet-reactive T cells, the numbers of $CD4^+$ T cells specific for an islet autoantigen (21) in mice cured with anti–IL-7Rα antibodies were identified with BDC2.5 pMHC class II tetramers (22). Similar numbers of tetramer-positive cells were found in the secondary lymphoid organs (Fig. 2*D*) of anti–IL-7Rα–treated vs. new-onset diabetic mice. This observation also held up for islet-specific $CD8^+$ T cells detected with NRPV7 pMHC class I tetramers [new-onset diabetic: $1.8 \times 10^6 \pm 7.4 \times 10^5$ lymph node (LN) and $6.4 \times 10^5 \pm 1.9 \times 10^5$ spleen (SP); anti–IL-7Rα/cured: $1.2 \times 10^6 \pm 6.5 \times 10^5$ (LNs) and $4.2 \times 10^5 \pm 6.6 \times 10^4$ (SP)]. These results demonstrate that considerable numbers of islet-reactive T cells remain present in anti–IL-7Rα–treated mice, indicating that poor $T_{E/M}$ cell survival is not the main mechanism for the therapeutic effect and suggesting that absence of IL-7 induces tolerance in the remaining diabetogenic T cells.

Blocking IL-7 Signals Increases Cell-Intrinsic and Cell-Extrinsic Inhibition of $CD4^+$ T Cells. Two major tolerance mechanisms known to control pathogenesis in the NOD diabetes model are the cell-intrinsic inhibitory pathway PD-1/PD-L1 (8–10) and $Foxp3^+$ Tregs (23). Therefore, we analyzed the impact of IL-7Rα blockade on the presence of PD-1–expressing $CD4^+$ T cells

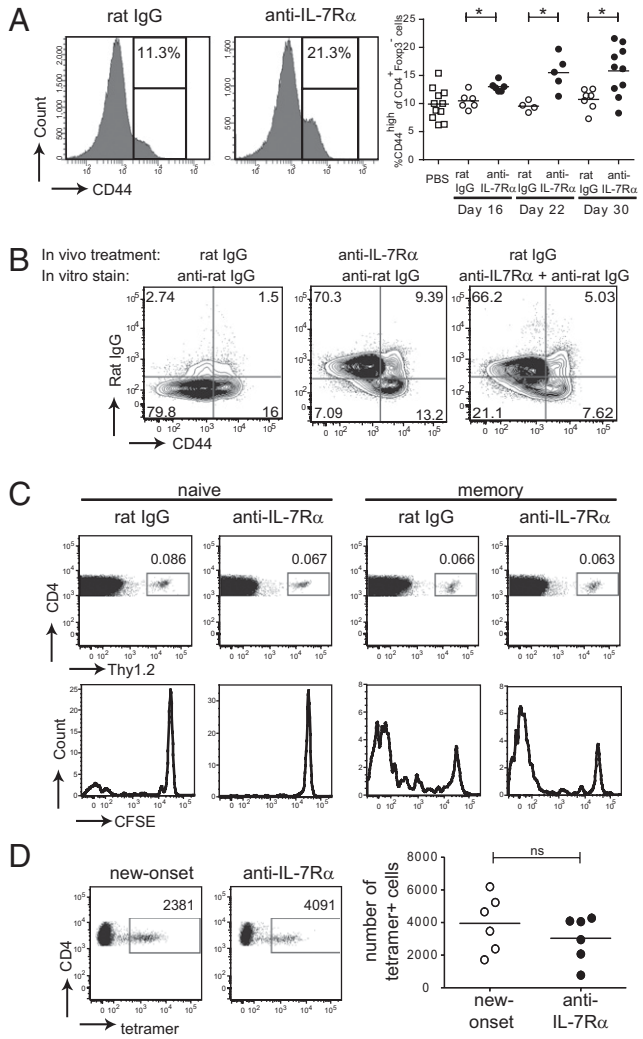

Fig. 2. IL-7Rα blockade does not preferentially deplete islet-reactive $T_{E/M}$ cells. (*A*) Prediabetic NOD mice (10–12 wk) were treated twice a week with anti–IL-7Rα or rat IgG antibodies for the indicated periods of time and the percentage of $CD44^{high}$ cells within the $CD4^+Foxp3^-$ population in the PLNs was determined by flow cytometry. Representative histograms (*Left*) and pooled data from five independent experiments (*Right*) are shown. Each symbol represents an individual mouse. $*P \leq 0.05$. (*B*) NOD mice were treated for 4 wk, as indicated, and lymphoid organs were harvested and stained with anti-rat IgG antibodies. Dot plots show the presence of anti–IL-7Rα antibodies on the cell surface of $CD44^{high}$ and $CD44^{low}$ $CD25^-CD4^+$ T cells from PLNs. Results are representative for two independent experiments (n = 3–4 mice per group). (*C*) 7.5×10^5 CFSE-labeled $CD44^{low}$ (naïve) or $CD44^{high}$ (memory) $CD4^+Thy1.2^+$ T cells were transferred to NOD.Thy1.1 recipients and treated with rat IgG or anti–IL-7Rα. Dot plots show percentage of $CD4^+Thy1.2^+$ cells present within the $CD4^+$ population in the PLNs after 4 wk of treatment and histograms show CFSE dilution, as a measure of cell division, in transferred cells. Data are representative of two independent experiments (n = 2 mice per group). (*D*) Quantification of islet antigen-specific $CD4^+$ T cells present in the lymphoid organs of new-onset and anti–IL-7Rα-cured mice from Fig. 1*E*, determined by BDC2.5-reactive tetramer staining and flow cytometry; ns, not significant.

and Tregs in NOD mice. After 2–3 wk of treatment, the percentage of both $PD\text{-}1^+Foxp3^{neg}$ cells and $Foxp3^+$ Tregs was increased within the $CD4^+$ T-cell population (Fig. 3 *A*–*C*). Absolute numbers of $PD\text{-}1^+$ cells also increased in the draining lymphoid organs, albeit less significantly because of the overall decrease in total $CD4^+$ T-cell numbers (Fig. S1*C*). Average $PD\text{-}1^+Foxp3^{neg}$ cell counts 16 d after anti–IL-7Rα vs. rat IgG administration were respectively 295,322 vs. 231,716 (PLN), 150,529 vs. 268,323 (ILN), and 1,742,726 vs. 1,523,309 (spleen). Average Treg counts in anti–IL-7Rα vs. rat IgG-treated animals were 414,637 vs. 383,071 (PLN), 392,669 vs. 538,038 (ILN), and 2,170,155 vs. 2,879,718 (spleen). Because PD-1 expression is known to be induced after T-cell activation (24), it was not surprising that anti–IL-7Rα–mediated increases in PD-1 were largely limited to the $CD44^{high}$ $T_{E/M}$ population (Fig. 3*D*). Enhanced numbers of Tregs after IL-7R blockade have been reported previously (25) and can be attributed to lower IL-7Rα expression in this population, and hence reduced dependency on IL-7 for survival. Although Tregs did not contribute to the therapeutic effect of IL-7Rα blockade in experimental autoimmune encephalitis (EAE) (25), increasing Treg numbers in NOD mice with IL-2 has been shown to prevent and reverse diabetes (23, 26). Hence, altering the balance of Treg/$T_{E/M}$ with anti–IL-7Rα antibodies likely strengthened cell-extrinsic regulation of pathogenic T cells and contributed to the therapeutic effect. To definitively determine the contribution of Tregs to anti–IL-7Rα–mediated protection, it would be necessary to restore the percentage of Tregs to the same level as rat IgG-treated control mice. However, current methods to reduce Treg numbers in vivo

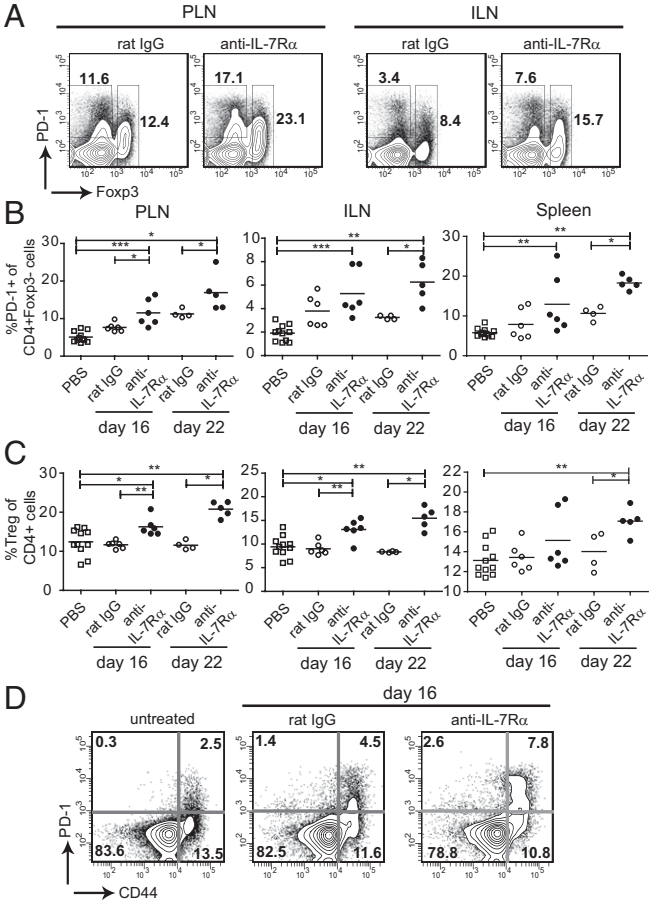

Fig. 3. Absence of IL-7 signals increases numbers of $PD\text{-}1^+$ and $Foxp3^+CD4^+$ T cells. Prediabetic NOD mice (10–12 wk) were treated with anti–IL-7Rα or rat IgG antibodies for 16–22 d and the PLNs and ILNs and spleen were stained for CD4, Foxp3, and PD-1. (*A*) Dot plots show the gates used to determine the percentages (values indicated) of $CD4^+Foxp3^+$ Tregs, and $PD\text{-}1^+$ cells within the $CD4^+Foxp3^-$ T-cell population. (*B* and *C*) Summary of percentages of $PD\text{-}1^+$ and $Foxp3^+$ $CD4^+$ T cells, respectively. Each symbol represents an individual mouse. Data are pooled from three independent experiments. $*P \leq 0.05$; $**P \leq 0.005$; $***P \leq 0.0005$. (*D*) Dot plots show representative PD-1 staining on naïve ($CD44^{low}$) and memory ($CD44^{high}$) $CD4^+Foxp3^{neg}$ T cells.

do not allow sufficiently accurate manipulation to achieve closely matching Treg numbers.

To ask whether the PD-1 pathway continues to provide protection during anti–IL-7Rα–mediated disease reversal, we treated a cohort of new-onset diabetic mice with anti–IL-7Rα mAbs and, once cured, asked if blocking the PD-1/PD-L1 pathway would restore the disease. The rapid relapse (~4–5 d) seen after administration of anti–PD-L1 antibodies (Fig. S2) demonstrates that even under the cover of anti–IL-7Rα antibody treatment, the presence of PD-1 on diabetogenic $T_{E/M}$ remains essential and suggests that increases in PD-1 expression are a powerful mechanism underlying the therapeutic effect. Because anti–PD-L1 also rapidly induces diabetes in untreated NOD mice however (9), it is not feasible to unequivocally prove the role of PD-1 in our therapeutic model.

IL-7 Counteracts PD-1–Mediated Tolerance in $T_{E/M}$ Cells. To understand the functional consequences of blocking IL-7 signals in T cells, we isolated $CD4^+$ T cells from NOD mice that were treated with anti–IL-7Rα mAb or control Abs and evaluated cytokine production after ex vivo restimulation. We found that IFN-γ production was severely impaired after 10 d of IL-7Rα blockade (Fig. 4*A*). Interestingly, IL-17 and IL-2 production were much less affected, suggesting IL-7 is mainly required for the Th1 response (Fig. 4*A*). Next, we directly compared the diabetogenic capacity of $CD4^+$ $T_{E/M}$ cells isolated from anti–IL-7Rα–treated and control mice by adoptively transferring equal numbers of these cells to NOD.SCID recipients and following diabetes incidence, without further treatment of the recipients. Strikingly, $CD4^+$ $T_{E/M}$ cells isolated from IL-7Rα–treated NOD mice failed to transfer diabetes to NOD.SCID recipients, unlike transferred control cells (Fig. 4*B*). Total $CD4^+$ T cells (excluding $CD25^+$ cells to eliminate Tregs) isolated from anti–IL-7Rα–treated and control mice behaved similarly, albeit with much slower kinetics (Fig. 4*C*). The failure of these cell populations to cause diabetes was not a result of poor survival or "grafting" after adoptive transfer, because equal numbers of memory T cells were recovered from the lymphoid organs 8–10 wk later (Fig. S3*A*). Furthermore, similar numbers of Tregs developed in recipients of treated vs. control $CD4^+$ T cells (Fig. S3*B*), indicating that cell-intrinsic regulation of $T_{E/M}$ cells plays an important role in anti–IL-7Rα–mediated therapy. In support of this, PD-L1 blockade accelerated diabetes onset in NOD.SCID mice that received $CD4^+T_{E/M}$ cells isolated from anti–IL-7Rα–treated mice (Fig. 4*D*), demonstrating that increased cell-intrinsic, PD-1–dependent inhibition of islet-reactive cells contributed to their loss of pathogenicity.

To directly demonstrate a causal relationship between IL-7 signaling and absence of PD-1 expression, we isolated naïve $CD4^+PD\text{-}1^{neg}$ T cells from NOD mice and stimulated these cells in vitro with anti-CD3 and anti-CD28 antibodies in the absence or presence of recombinant IL-7. We found that IL-7 diminished PD-1 expression on activated T cells in a dose-dependent manner (Fig. 5 *A* and *C*). Although PD-1 was initially induced in IL-7–containing cultures, further increases in surface expression of the receptor at the later stages of the response (days 4–6) were suppressed in the presence of the cytokine (Fig. 5 *B* and *C*). This activity of IL-7 was not limited to NOD T cells, because T-cell receptor Tg T cells from DO.11 mice responded similarly (Fig. S4). IL-7 may thus directly control PD-1 expression. It is noteworthy here that $Jak3^{-/-}$ T cells, which are impaired in transducing signals from IL-7 and other γc cytokines, show enhanced PD-1 expression after activation (27). $CD4^+$ T cells activated in the presence of IL-7 also showed increased functional competence, as demonstrated by enhanced IFN-γ production upon restimulation on day 6 (Fig. 5*D*); this result further underscores an important role for IL-7 in the promotion of Th1 responses.

Finally, to ask if a correlation exists between PD-1 and human type 1 diabetes, we compared PD-1 expression on $CD4^+$ T cells from peripheral blood of diabetic patients vs. healthy controls. Interestingly, diabetic patients showed a decreased

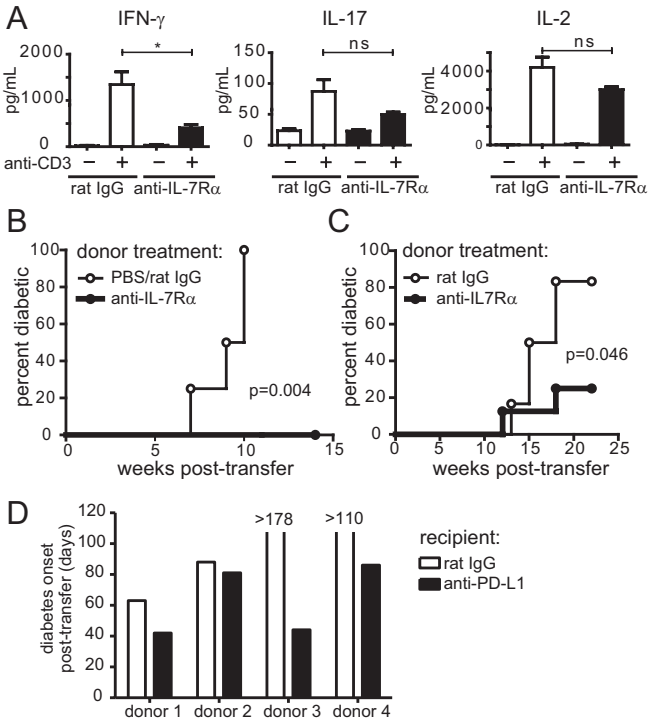

Fig. 4. $CD4^+$ T cells isolated from anti–IL-7Rα-treated mice lose effector function and diabetogenicity. (*A*) Prediabetic NOD mice were treated for 10 d with anti–IL-7Rα antibodies or rat IgG and 1×10^5 $CD4^+$ T cells isolated from lymph nodes and spleen were restimulated with anti-CD3 (1 μg/mL) and bone marrow-derived dendritic cells (1×10^5) for 15 h. Supernatants were collected and cytokines detected by ELISA. Results are pooled from two independent experiments ($n = 6$). $^*P \le 0.05$; $^{***}P \le 0.0005$; ns, not significant. (*B*) $CD25^-CD44^{high}CD4^+$ $T_{E/M}$ cells were isolated from lymph nodes and spleen of anti–IL-7Rα– ($n = 5$) or control-treated ($n = 4$) nondiabetic NOD mice and 2.5×10^5 (experiment 1) or 1.2×10^6 (experiment 2) cells from individual donors were transferred to NOD.SCID recipients. Diabetes incidence was followed without further antibody treatment of the recipients. Graph shows pooled data from two independent experiments. $P = 0.004$. (*C*) Total $CD25^-CD4^+$ T cells were isolated from prediabetic (14-wk-old) NOD mice that were treated for 2–4 wk with anti–IL-7Rα ($n = 8$) or rat IgG ($n = 6$) and 3.7×10^6 cells from individual mice were transferred to NOD.SCID recipients and diabetes incidence followed in the absence of further antibody treatment. Graph shows pooled data from two independent experiments. $P = 0.046$. (*D*) $CD44^{high}$ $CD4^+$ $T_{E/M}$ cells were isolated from new-onset diabetic NOD mice that were cured with anti–IL-7Rα blockade, as in Fig. 1*D*. The 5×10^5 $T_{E/M}$ cells isolated from each individual donor were split in two and adoptively transferred to two NOD.SCID recipients. Matching recipients were treated with rat IgG or anti–PD-L1 antibodies and graph shows days to diabetes onset for each individual treated vs. control pair. Mice that did not become diabetic were killed on the indicated days. $P < 0.0001$.

presence of $PD\text{-}1^+$ $CD45RA^-$ memory T cells (Fig. S5). These data suggest that some of these $PD\text{-}1^-$ antigen-experienced cells may be islet-specific, providing a rationale for developing methods to increase expression of the inhibitory molecule PD-1 in diabetes patients.

Discussion

Although interfering with T-cell receptor and costimulatory signals required for activation of naïve self-reactive T cells has been successful to prevent autoimmunity in some models (28), it has typically not been effective once disease is established. One suspected reason for this failure is that $T_{E/M}$ cells may be the main pathogenic cells perpetuating the response. Memory cells are much less dependent on costimulatory signals for their activation (29), making them difficult to control and underscoring the need for novel approaches to target these cells. Importantly, memory

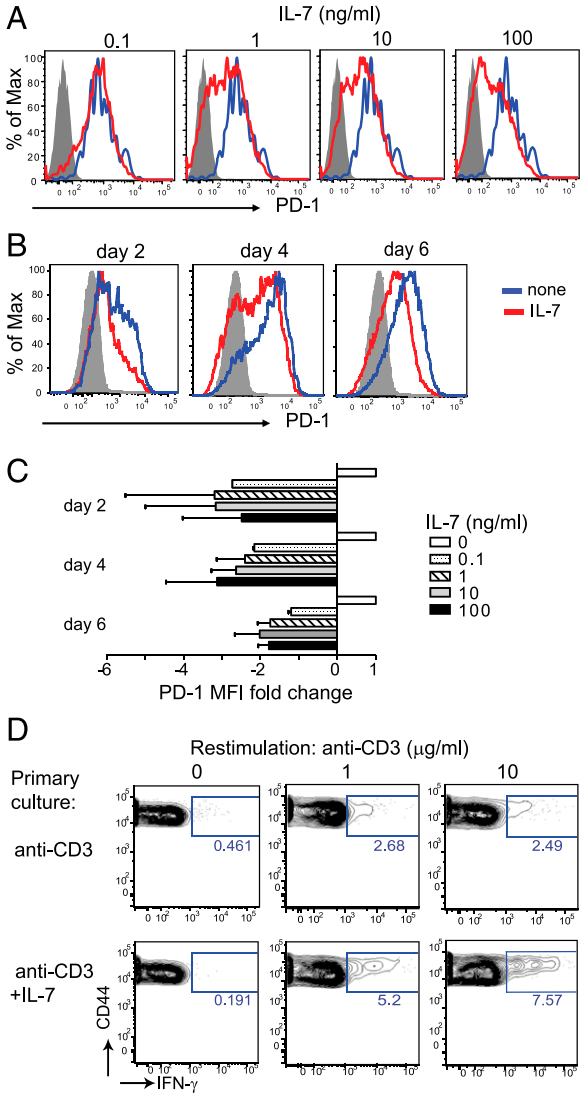

Fig. 5. IL-7 inhibits PD-1 expression in vitro. Naïve PD-1^{-}Foxp3^{-}CD4^{+} T cells (gray, filled) were isolated from NOD/Foxp3-GFP mice and stimulated in vitro with anti-CD3 (10 μg/mL) + anti-CD28 (1 μg/mL) antibodies with (red) or without (blue) the indicated amounts of recombinant IL-7. (*A*) Histograms show PD-1 expression on activated (CD44^{high}) T cells in the presence of increasing amounts of IL-7 and (*B*) at different times after stimulation with and without IL-7 (10 ng/mL). (*C*) Graph shows fold change in mean fluorescent intensity (MFI) of PD-1 staining relative to the normalized value (= 1) of cultures without IL-7. Data are pooled from four independent experiments. (*D*) Cells were stimulated for 6 d with or without IL-7 (10 ng/mL), as in *A* and, after harvesting and washing, restimulated with anti-CD3 mAb and splenocytes for 18 h (in the presence of BFA for the last 5 h). Dot plots show IFN-γ production determined by intracellular cytokine staining. Results are representative for two independent experiments.

T cells are critically dependent on instructive signals from specific cytokines, such as IL-7, for their generation and maintenance (18, 20, 30); hence, interfering with these proteins may represent a strategy for treating autoimmune disease.

In this study we show that treatment of NOD mice with anti–IL-7Rα mAbs can prevent and cure diabetes. Importantly, this effect was not a result of preferential depletion of memory or antigen-specific diabetogenic T cells. Because $T_{E/M}$ cells isolated from anti–IL-7Rα–treated mice were unable to transfer disease to NOD.SCID recipients, the treatment works through inducing a mechanism of cell-intrinsic tolerance that could be transferred to a new host, independent of Tregs. $T_{E/M}$ cells present in animals after anti–IL-7Rα treatment expressed increased levels of the inhibitory receptor PD-1, and inhibiting the interaction of PD-1 with its ligand PD-L1 restored disease in cured mice, providing a strong correlation between this critical inhibitory mechanism and therapeutic efficacy. Because IL-7Rα is also part of the heterodimeric receptor for thymic stromal lymphopoietin, it cannot be excluded that anti–IL-7Rα antibodies also compromise some functions of this cytokine in vivo. However, thymic stromal lymphopoietin has been described as protective for autoimmune diabetes in NOD mice (31).

Recent studies are starting to reveal novel, specific functions of IL-7 in T-cell responses. Liu et al. showed that blockade of IL-7 at the onset of EAE resulted in reduction of disease severity because of a selective reduction of IL-17 production (25). This is likely not the mechanism of disease reversal in NOD mice, as Th17 cells are not considered the pathogenic population in this model. In fact, Th17-skewed BDC2.5 transgenic effector cells become IFN-γ–producing Th1 cells after transfer to NOD.SCID mice and inhibition of IL-17 does not prevent diabetes in this transfer model (32). Our data, in accordance with a recent study on EAE (33), suggest that IL-7 blockade mainly affects Th1 cells (Figs. 4 and 5). We propose that Th1-skewed $T_{E/M}$ cells become dysfunctional in the absence of IL-7 signals and increased expression of PD-1 is one cell-intrinsic inhibitory mechanism underlying their inability to secrete IFN-γ. Thus, our data may be related to recent observations showing that administration of a high dose of IL-7 enhances antitumor and antiviral responses by counteracting inhibitory mechanisms in T cells (3, 4). In addition, our study indicates that under physiological conditions, IL-7 reduces PD-1 expression and maintains $T_{E/M}$ cells in a functionally responsive state by regulating their antigen responsiveness.

The expression of PD-1 on CD8^{+} memory T cells has been widely reported in the setting of chronic virus infections, such as HIV, and hepatitis B and C viruses, where antigen exposure is prolonged because the infection is not effectively cleared (24, 34). Blockade of PD-1/PD-L1 interaction results in increased numbers of cytokine-producing virus-specific CD8^{+} T cells and a reduction in viral titers (7). Therefore, PD-1 expression on memory CD8^{+} T cells has been a feature of functional impairment or exhaustion. Although exhaustion of memory CD4^{+} T cells has not been described, we propose that autoimmune settings give rise to such a population, because autoreactive T cells are also chronically exposed to antigen. Interestingly, exhausted memory T cells show low IL-7Rα expression (35), and we speculate that a causal relation exists between the absence of IL-7 signals and the up-regulation of PD-1. In autoimmune diabetes, changing levels of IL-7 in the draining PLNs or in the pancreas itself, perhaps induced by inflammation (36), may allow a fraction of islet-reactive $T_{E/M}$ cells to escape PD-1–mediated control and cause tissue damage. The rapid reversal of hyperglycemia we observe after anti–IL-7Rα administration in new-onset diabetic mice certainly indicates effects of the treatment in the pancreas. This result is feasible because it has been demonstrated that PD-L1 is expressed on the β-cells (5) and, hence, induction of PD-1 in the infiltrating pathogenic T cells could provide immediate protection from further islet loss.

We have exploited the idea that IL-7 plays a critical role in the pathogenesis of autoimmune diabetes to test the therapeutic efficacy of IL-7Rα blockade in established disease. We show that this approach to induce PD-1–dependent tolerance may be successful for the treatment of autoimmune diseases, by itself or in combination with other tolerance-inducing strategies. Importantly, Tregs, which represent another powerful mechanism of peripheral tolerance, are less sensitive to IL-7 deprivation because of low expression of IL-7Rα (25). This finding is reflected in a proportional increase of Tregs within the CD4^{+} T-cell population after IL-7Rα blockade, and is likely an added benefit to this therapy. Finally, it should be noted that Tregs typically express higher levels of PD-1 than naïve T cells and it may be of interest to investigate whether this is related to decreased IL-7 signaling.

In conclusion, our data show that physiologic levels of IL-7 contribute to the pathogenesis of autoimmune disease in a model of spontaneous diabetes development in lymphosufficient animals, and suggest that a previously unrecognized link between IL-7 and the PD-1/PD-L1 tolerance pathway underlies IL-7's role in autoimmunity.

Materials and Methods

Mice. Female NOD mice were purchased from The Jackson Laboratory or Taconic. NOD.SCID, NOD.Thy1.1, NOD/Foxp3GFP (37), and DO.11.10 mice were bred in our facility. All animal experiments were approved by the Institutional Animal Care and Use Committee of the University of California at San Francisco.

Antibody Treatments. Anti–IL-7Rα (A7R34) and anti–PD-L1 (MIH5) antibodies for in vivo blocking experiments were produced by the hybridoma cell lines and purified in our laboratory. Rat IgG was used as a control. For IL-7Rα blockade experiments, 0.5 mg anti–IL-7Rα was administered twice weekly intraperitoneally. Organs were harvested for analysis 2–3 d after the last antibody administration. Anti–PD-L1 antibodies were given as described previously (10). Further details can be found in *SI Materials and Methods*.

Diabetes Assessment and Histology. Diabetes incidence was followed by urine analysis and measuring of blood-glucose levels. Mice with two consecutive readings between 250 and 400 mg/dL were considered new-onset diabetic and used for experiments attempting to reverse the disease. Histological analysis was performed by fixing pancreata in formalin and staining sections with H&E; 10 sections per pancreas were blindly scored for insulitis (0 = no infiltrate, 1 = 0–25%, 2 = 25–75%, 3 = > 75%). Further details can be found in *SI Materials and Methods*.

Tetramer Staining, Flow Cytometry, Cell Sorting, and Adoptive Transfers. Islet antigen-specific T cells present in secondary lymphoid organs were detected after enrichment with BDC2.5 pMHC tetramers (National Institutes of Health tetramer core facility) following a method described previously (22). Phenotypic analysis of cell populations was performed by multiparameter flow cytometry using fluorescently labeled antibodies. For adoptive transfer studies and in vitro experiments, naïve ($CD25^{neg}CD44^{low}$IL-$7R\alpha^{high}$) and memory ($CD25^{neg}CD44^{high}$IL-$7R\alpha^{high}$) $CD4^+$ T cells from donors were labeled with antibodies and isolated with a high-speed cell sorter (MoFlo, DakoCytomation). Further details can be found in *SI Materials and Methods*.

In Vitro Stimulation and Cytokine Assays. Naive PD-$1^{neg}$$Foxp3^{neg}$ $CD4^+$ T cells were isolated from NOD/Foxp3 GFP mice and stimulated with anti-CD3 and anti-CD28 antibodies in the presence or absence of recombinant murine IL-7. Cytokine production was determined by ELISA or intracellular cytokine staining and flow cytometry. Further details can be found in *SI Materials and Methods*.

Statistics. Statistically significant differences between groups were determined using the Mantel–Cox log-rank test (for diabetes incidence), one-tailed Mann–Whitney *U* test (for cell numbers and percentages), two-tailed unpaired *t* test (for cytokine assays), and χ^2 test (for Fig. 4*D*). Horizontal bars in graphs indicate statistical significance ($P < 0.05$) and *P* values are indicated.

ACKNOWLEDGMENTS. We thank Shuwei Jiang for expert cell sorting, Navdeep Grewal for histology, and Carlos Benitez for mouse husbandry. This study was supported by Juvenile Diabetes Research Foundation Grant 32-2008-354 (to H.D.); National Institute of General Medical Sciences Grant 1 R25 GM56847 (to C.P.); and National Institutes of Health Grants R37 AI46643 (to J.A.B.) and P30 DK063720 (University of California at San Francisco-Diabetes and Endocrinology Research Center).

1. Bluestone JA, Herold K, Eisenbarth G (2010) Genetics, pathogenesis and clinical interventions in type 1 diabetes. *Nature* 464:1293–1300.
2. Surh CD, Sprent J (2008) Homeostasis of naive and memory T cells. *Immunity* 29: 848–862.
3. Pellegrini M, et al. (2009) Adjuvant IL-7 antagonizes multiple cellular and molecular inhibitory networks to enhance immunotherapies. *Nat Med* 15:528–536.
4. Pellegrini M, et al. (2011) IL-7 engages multiple mechanisms to overcome chronic viral infection and limit organ pathology. *Cell* 144:601–613.
5. Keir ME, et al. (2006) Tissue expression of PD-L1 mediates peripheral T cell tolerance. *J Exp Med* 203:883–895.
6. Keir ME, Butte MJ, Freeman GJ, Sharpe AH (2008) PD-1 and its ligands in tolerance and immunity. *Annu Rev Immunol* 26:677–704.
7. Barber DL, et al. (2006) Restoring function in exhausted CD8 T cells during chronic viral infection. *Nature* 439:682–687.
8. Wang J, et al. (2005) Establishment of NOD-Pdcd1-/- mice as an efficient animal model of type I diabetes. *Proc Natl Acad Sci USA* 102:11823–11828.
9. Ansari MJ, et al. (2003) The programmed death-1 (PD-1) pathway regulates autoimmune diabetes in nonobese diabetic (NOD) mice. *J Exp Med* 198:63–69.
10. Fife BT, et al. (2006) Insulin-induced remission in new-onset NOD mice is maintained by the PD-1-PD-L1 pathway. *J Exp Med* 203:2737–2747.
11. Fife BT, et al. (2009) Interactions between PD-1 and PD-L1 promote tolerance by blocking the TCR-induced stop signal. *Nat Immunol* 10:1185–1192.
12. Shoda LK, et al. (2005) A comprehensive review of interventions in the NOD mouse and implications for translation. *Immunity* 23:115–126.
13. Sudo T, et al. (1993) Expression and function of the interleukin 7 receptor in murine lymphocytes. *Proc Natl Acad Sci USA* 90:9125–9129.
14. Seddon B, Tomlinson P, Zamoyska R (2003) Interleukin 7 and T cell receptor signals regulate homeostasis of CD4 memory cells. *Nat Immunol* 4:680–686.
15. You SMB, et al. (2005) Autoimmune diabetes onset results from qualitative rather than quantitative age-dependent changes in pathogenic T-cells. *Diabetes* 54:1415–1422.
16. Lepault F, Gagnerault MC, Faveeuw C, Bazin H, Boitard C (1995) Lack of L-selectin expression by cells transferring diabetes in NOD mice: Insights into the mechanisms involved in diabetes prevention by Mel-14 antibody treatment. *Eur J Immunol* 25:1502–1507.
17. Flynn JC, McInerney MF (2000) High density insulin receptor-positive diabetogenic T lymphocytes in nonobese diabetic mice are memory cells. *Immunopharmacol Immunotoxicol* 22:387–400.
18. Li J, Huston G, Swain SL (2003) IL-7 promotes the transition of CD4 effectors to persistent memory cells. *J Exp Med* 198:1807–1815.
19. Moulton VR, Bushar ND, Leeser DB, Patke DS, Farber DL (2006) Divergent generation of heterogeneous memory CD4 T cells. *J Immunol* 177:869–876.
20. Dooms H, Wolslegel K, Lin P, Abbas AK (2007) Interleukin-2 enhances CD4+ T cell memory by promoting the generation of IL-7R alpha-expressing cells. *J Exp Med* 204: 547–557.
21. Stadinski BD, et al. (2010) Chromogranin A is an autoantigen in type 1 diabetes. *Nat Immunol* 11:225–231.
22. Moon JJ, et al. (2009) Tracking epitope-specific T cells. *Nat Protoc* 4:565–581.
23. Tang Q, et al. (2008) Central role of defective interleukin-2 production in the triggering of islet autoimmune destruction. *Immunity* 28:687–697.
24. Sharpe AH, Wherry EJ, Ahmed R, Freeman GJ (2007) The function of programmed cell death 1 and its ligands in regulating autoimmunity and infection. *Nat Immunol* 8: 239–245.
25. Liu X, et al. (2010) Crucial role of interleukin-7 in T helper type 17 survival and expansion in autoimmune disease. *Nat Med* 16:191–197.
26. Grinberg-Bleyer Y, et al. (2010) IL-2 reverses established type 1 diabetes in NOD mice by a local effect on pancreatic regulatory T cells. *J Exp Med* 207:1871–1878.
27. Mayack SR, Berg LJ (2006) Cutting edge: An alternative pathway of CD4+ T cell differentiation is induced following activation in the absence of gamma-chain-dependent cytokine signals. *J Immunol* 176:2059–2063.
28. Howard LM, Kohm AP, Castaneda CL, Miller SD (2005) Therapeutic blockade of TCR signal transduction and co-stimulation in autoimmune disease. *Curr Drug Targets Inflamm Allergy* 4:205–216.
29. London CA, Lodge MP, Abbas AK (2000) Functional responses and costimulator dependence of memory CD4+ T cells. *J Immunol* 164:265–272.
30. Kondrack RM, et al. (2003) Interleukin 7 regulates the survival and generation of memory CD4 cells. *J Exp Med* 198:1797–1806.
31. Besin G, et al. (2008) Thymic stromal lymphopoietin and thymic stromal lymphopoietin-conditioned dendritic cells induce regulatory T-cell differentiation and protection of NOD mice against diabetes. *Diabetes* 57:2107–2117.
32. Bending D, et al. (2009) Highly purified Th17 cells from BDC2.5NOD mice convert into Th1-like cells in NOD/SCID recipient mice. *J Clin Invest* 119:565–572.
33. Lee LF, et al. (2011) IL-7 promotes T(H)1 development and serum IL-7 predicts clinical response to interferon-β in multiple sclerosis. *Sci Transl Med* 3:93ra68.
34. Day CL, et al. (2006) PD-1 expression on HIV-specific T cells is associated with T-cell exhaustion and disease progression. *Nature* 443:350–354.
35. Wherry EJ, et al. (2007) Molecular signature of CD8+ T cell exhaustion during chronic viral infection. *Immunity* 27:670–684.
36. Sawa Y, et al. (2009) Hepatic interleukin-7 expression regulates T cell responses. *Immunity* 30:447–457.
37. Zhou X, et al. (2009) Instability of the transcription factor Foxp3 leads to the generation of pathogenic memory T cells in vivo. *Nat Immunol* 10:1000–1007.

Supporting Information

Penaranda et al. 10.1073/pnas.1203692109

SI Materials and Methods

Mice. Female nonobese diabetic (NOD) mice were purchased from The Jackson Laboratory or Taconic. NOD.SCID, NOD.Thy1.1, NOD/Foxp3GFP (1), and DO.11.10 mice were bred in the authors' facility. Mice were housed in the specific pathogen-free facility of the University of California at San Francisco and all animal experiments were approved by the Institutional Animal Care and Use Committee of the University of California at San Francisco.

Diabetes Assessment and Histology. Diabetes incidence was followed by urine analysis (Diastix; Bayer) and measuring of blood-glucose levels with a Contour glucose meter (Bayer). Mice with two consecutive readings between 250 and 400 mg/dL were considered new-onset diabetic and used for anti–IL-7 receptor-α (IL-7Rα) treatment. Histological analysis was performed by fixing pancreata in 10% (vol/vol) buffered formalin and staining 5-μm sections with H&E; 10 sections per pancreas were blindly scored for insulitis. Scores are as follows: 0 = no infiltrate, 1 = 0–25%, 2 = 25–75%, 3 = > 75%. Digital images were captured with an Optiphot microscope equipped with an Axiocam digital camera and analyzed using Adobe Illustrator CS2.

Antibody Treatment. Anti–IL-7Rα (rat IgG2a, clone A7R34) and anti–PD-L1 (Programmed Death-1 ligand) (rat IgG2a, clone MIH5) antibodies for in vivo blocking experiments were produced by the hybridoma cell lines and purified with Protein G Sepharose 4 Fast Flow (GE Healthcare) in our laboratory. Rat IgG (Jackson ImmunoResearch Laboratories) was used as a control. For IL-7Rα blockade, 0.5-mg anti–IL-7Rα antibodies in PBS were administered twice weekly intraperitoneally. Anti–PD-L1 antibodies were given as described previously (2).

Antibodies. Fc receptors were blocked with anti-CD16/CD32 antibodies, prepared in our laboratory from the hybridoma cell line, before all antibody staining procedures. The following antibodies coupled to the indicated fluorochromes were used for detection of murine activation markers and cytokine receptors: anti–CD3ε-Pacific Blue (17A2; eBioscience); anti–CD4-PerCP (RM4-5; BD) or –Alexa-700 (eBioscience); anti–CD8-PercP (53-6.7; BD); anti–CD11b-FITC (M1/70; BD); anti–CD11c-FITC (HL3; BD); anti–CD25-FITC, -APC (7D4; BD) or –APC-eFluor780 (PC61; eBioscience); anti–CD44-APC or –APC-eFluor780 (IM7; eBioscience); anti-CD45R/B220 (RA3-6B2; eBioscience); anti–CD127-biotin (A7R34; eBioscience); CD90.1-PercP (OX-7; BD); CD90.2-PercP (30-H12; Biolegend); CD279-PE (J43; eBioscience) or –PE-Cy7 (RMP1-30; Biolegend); anti–FoxP3-FITC (FJK-16s; eBioscience); polyclonal anti-rat Ig (BD); streptavidin-PE and -APC (eBioscience); Armenian hamster control IgG2 PE (BD).

Tetramer Staining, Flow Cytometry, Cell Sorting, and Adoptive Transfers. Islet antigen-specific T cells present in secondary lymphoid organs were detected after enrichment with BDC2.5 pMHC tetramers [I-A^{g7} BDC 2.5 mimotope sequence 2 RTRPLWVRME (National Institutes of Health tetramer core facility)] following a method described previously (3). IGRP-specific $CD8^+$ T cells were identified by direct staining with NRPV7 tetramers [H-2K(d) sequence KYNKANVFL (National Institutes of Health tetramer core facility)]. Tetramer-positive cells were quantified using percentages obtained by flow cytometry and absolute counts of (enriched) cells. Phenotypic analysis of cell populations was performed by multiparameter flow cytometry. Fluorescence intensities were measured on an LSRII or Fortessa flow cytometer and data were analyzed with FACSDiva (BD Biosciences) or FlowJo software. For adoptive transfer studies and in vitro experiments, naïve ($CD25^{neg}$ $CD44^{low}$) and $T_{E/M}$ ($CD25^{neg}CD44^{high}$) $CD4^+$ cells from donors were labeled with antibodies and isolated with a high-speed cell sorter (MoFlo, DakoCytomation). To track cell division in vivo, cells were labeled with carboxyfluorescein diacetate succinimidyl ester (CFSE) before adoptive transfer, following a previously described protocol (4).

In Vitro Stimulation and Cytokine Assays. Naïve PD-$l^{neg}Foxp3^{neg}$ $CD4^+$ T cells were isolated from NOD/Foxp3GFP mice and stimulated with 1–10 μg soluble anti-CD3 (145-2C11; BD) and 1 μg anti-CD28 (37.51; BD) antibodies in the presence or absence of recombinant murine IL-7 (Peprotech). Cells were cultured in RPMI 1640 media (Invitrogen) supplemented with 1 mM each of L-glutamine, nonessential amino acids, sodium pyruvate, Hepes, penicillin, streptomycin (Invitrogen), 50 μM 2-ME, and 10% FCS (Omega Scientific), and incubated at 37° in 5% CO_2. Cell cultures were set up in round-bottomed 96-well plates (BD Falcon) and harvested after 2, 4, and 6 d for flow cytometric analysis of PD-1 expression. Death cells were excluded from the analysis by staining with 4′6-diamidino-2-phenylindole (Invitrogen). Cytokine production after restimulation of the cells with anti-CD3 Ab and splenocytes [treated with mitomycin c (Sigma)] was determined by intracellular cytokine staining and flow cytometry; Brefeldin A (Epicentre) was added to the cultures for the final 4–5 h of the assay. To determine cytokine production by ex vivo restimulated cells from treated NOD mice, $CD4^+$ T cells were isolated from lymphoid organs using an EasySep $CD4^-$ selection kit (Stemcell Technologies) according to the manufacturer's instructions. Next, 1×10^5 purified $CD4^+$ T cells were cultured with anti-CD3 antibodies (1 μg/mL) and 1×10^5 NOD bone marrow-derived dendritic cells (generated as described in ref. 4) in round-bottomed 96-well plates. Duplicate cultures were set up and IL-2, IFN-γ, and IL-17 concentrations were determined in supernatants by ELISA, according to the manufacturer's instructions (BD PharMingen).

PD-1 Staining in Type 1 Diabetes Patients. Venous blood was drawn with ethical approval from patients attending the clinical type 1 diabetes service at the University Hospital Birmingham National Health Service Foundation Trust, United Kingdom. Patients had been clinically diagnosed with type 1 diabetes according to the 1997 American Diabetes Association guidelines. Venous blood was also drawn from healthy volunteers, matched as closely as possible for age and sex. Mononuclear cells were isolated from fresh blood samples by buoyant density centrifugation and analyzed by multicolor flow cytometry using antibodies against CD3, CD4, CD45RA, CD25, and PD-1. Data were acquired using a Cyan ADP Analyzer and processed using FlowJo software.

Statistics. Statistically significant differences between groups were determined using the Mantel–Cox log-rank test (for diabetes incidence), one-tailed Mann–Whitney *U* test (for cell numbers and percentages), two-tailed unpaired *t* test (for cytokine assays), and χ^2 test (for Fig. 4*D*) using Prism software. Horizontal bars in graphs indicate statistical significance ($P < 0.05$) and *P* values are indicated.

1. Zhou X, et al. (2009) Instability of the transcription factor Foxp3 leads to the generation of pathogenic memory T cells in vivo. *Nat Immunol* 10:1000–1007.
2. Fife BT, et al. (2006) Insulin-induced remission in new-onset NOD mice is maintained by the PD-1-PD-L1 pathway. *J Exp Med* 203:2737–2747.
3. Moon JJ, et al. (2009) Tracking epitope-specific T cells. *Nat Protoc* 4:565–581.
4. Dooms H, Wolslegel K, Lin P, Abbas AK (2007) Interleukin-2 enhances CD4+ T cell memory by promoting the generation of IL-7R alpha-expressing cells. *J Exp Med* 204: 547–557.

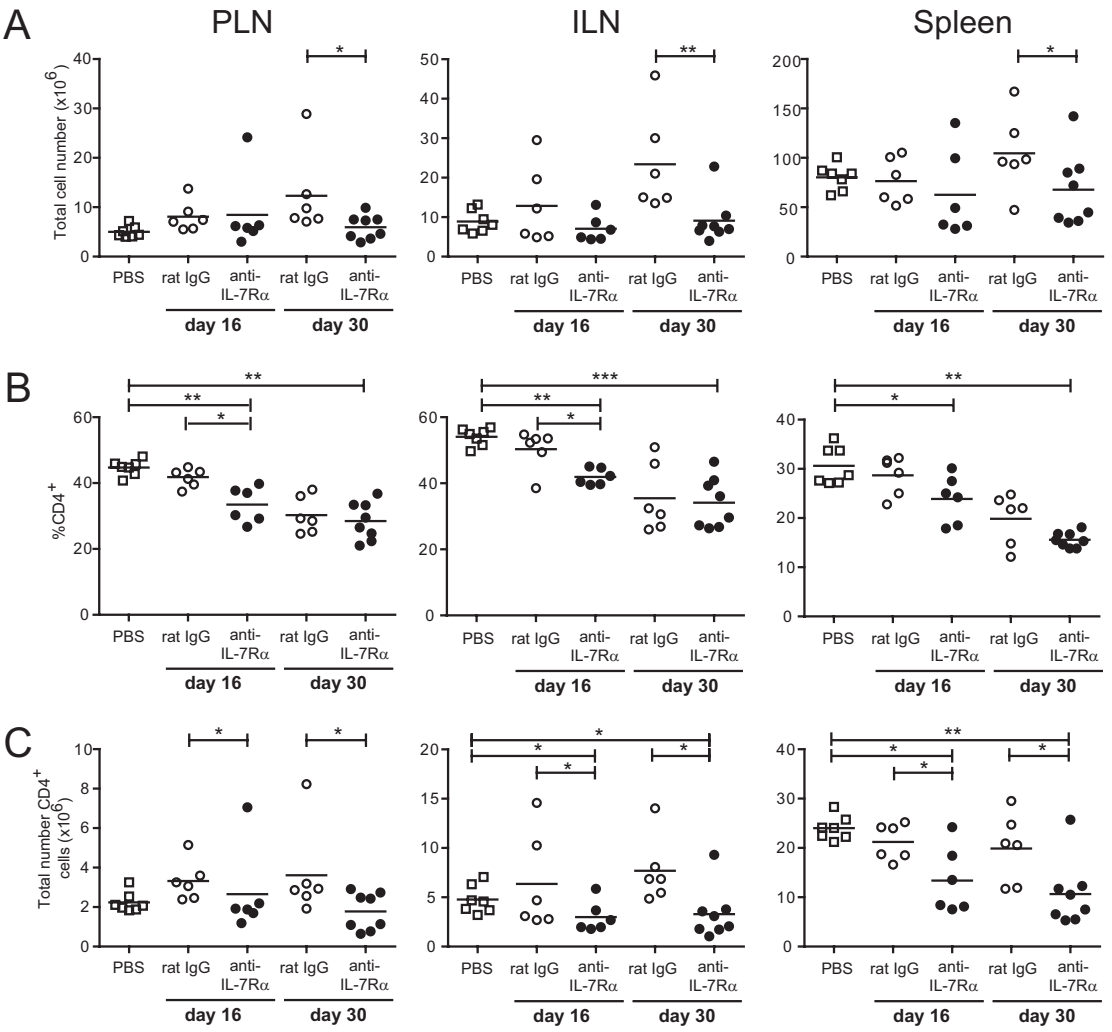

Fig. S1. Lymphocyte numbers after anti–IL-7Rα treatment. Prediabetic NOD mice (10–12 wk) were treated twice a week with anti–IL-7Rα or rat IgG antibodies for the indicated periods of time. (*A*) Total cell numbers, (*B*) percentage of $CD4^+$ T cells, and (*C*) $CD4^+$ T-cell numbers in pancreatic (PLN) and inguinal (ILN) lymph nodes and spleen are shown. Each symbol represents an individual mouse. Data are pooled from two independent experiments per timepoint. $*P \leq 0.05$; $**P \leq 0.005$; $***P \leq 0.0005$.

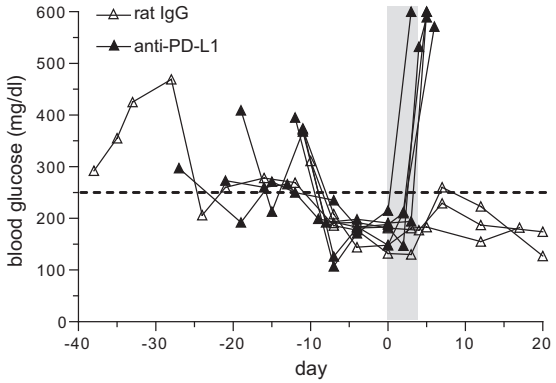

Fig. S2. The PD-1/PD-L1 pathway maintains tolerance after IL-7Rα blockade. New-onset diabetic NOD mice were treated as in Fig. 1*D*. Cured mice (three consecutive blood-glucose readings < 250 mg/dL for 1 wk) were treated with anti–PD-L1 antibodies or rat IgG every other day (starting on day 0; shaded area shows treatment period). Graph shows blood-glucose levels from individual mice.

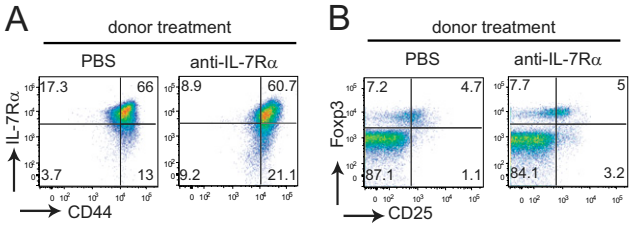

Fig. S3. CD4$^+$ T-cell survival and regulatory T cell (Treg) presence in adoptively transferred NOD.SCID mice. $T_{E/M}$ cells were isolated from anti–IL-7Rα or PBS-treated NOD donors, as in Fig. 4*B*, and transferred to NOD.SCID recipients. PLNs were harvested 8–10 wk later and histograms show (*A*) CD44^{high}IL-7Rα^{high} memory T cells and (*B*) Foxp3$^+$CD25$^+$ Tregs present within the CD4$^+$ T-cell gate. Dot plots are representative of three individual mice.

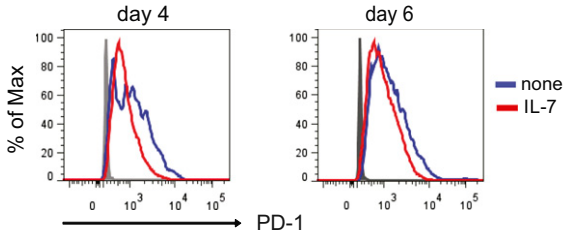

Fig. S4. IL-7 reduces PD-1 expression on activated CD4$^+$ DO.11 T cells. Naïve DO.11 T cells (filled histograms) were isolated from lymph nodes and spleens by high-speed cell sorting and stimulated in vitro, as in Fig. 5. Histograms show PD-1 expression on activated (CD44^{high}) T cells on day 4 and 6 after stimulation with (red) and without (blue) IL-7 (10 ng/mL).

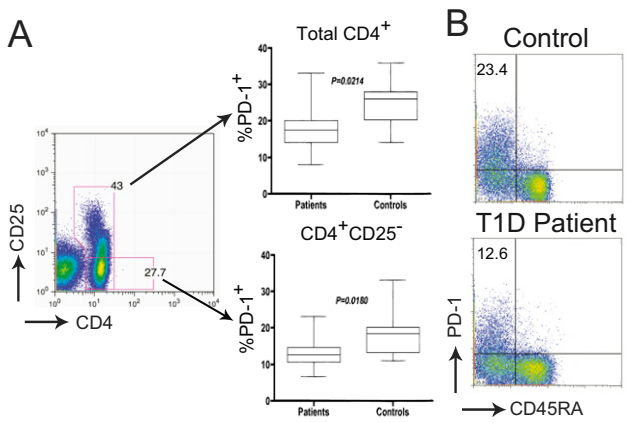

Fig. S5. Reduced PD-1 expression in type 1 diabetes patients. Fresh ex vivo peripheral blood mononuclear cells isolated from type 1 diabetes patients or healthy controls were analyzed by multicolor flow cytometry (see *SI Materials and Methods*). (*A*) Comparison of PD-1 staining on $CD4^+$ T cells from type 1 diabetes patients or healthy controls. The difference seen in the total $CD4^+$ population ($P = 0.0214$) is not attributable to PD-1 expression on Tregs because the difference is maintained after gating on $CD4^+CD25^-$ cells ($P = 0.0180$). Presented data derive from 16 type 1 diabetes patients and 13 healthy controls, with mean ages of 29 and 27, respectively. There was no correlation of PD-1 levels with donor age, hemoglobin A1C or blood-glucose levels. (*B*) Representative CD45RA staining on gated $CD4^+$ lymphocytes showing PD-1 expression is largely restricted to memory cells.